Detection of Voltage Fluctuations in Low-Voltage Power Distribution Networks with Principal Component Analysis

Laiz Souto, Ferran Torrent, Sergio Herraiz, Joaquim Melendez
Universitat de Girona, Spain
laiz.souto@gmail.com

SUMMARY

This work presents the development and results of an automated event detection strategy based on principal component analysis (PCA) for low voltage distribution grids with the presence of distributed generation (DG) and phasor measurement units (PMUs). The proposed methodology, relying on measurements provided by PMUs installed at different nodes, is capable of correctly identifying and distinguishing abnormal operating conditions (AOC) from normal operating conditions (NOC) without requiring any information about the network topology or electrical parameters of its components. Moreover, it is tested and validated under voltage sags and swells in a real-based power distribution network simulated in MATLAB with PMUs deployed in distinct settings.

INTRODUCTION

The increasing penetration level of renewable energy sources, storage systems, and new energy appliances is gradually changing the design and operation of electric power systems, while posing additional challenges to power system protection and power quality, particularly at distribution level, for the uncertain, dynamic, ever-changing nature of distributed energy resources[1] [2]. Consequently, additional measures are required to properly detect faults and handle voltage fluctuations caused by the intermittent nature of renewables and sudden, random, unpredictable changes in energy consumption patterns within the distribution grid[3] [4].

In this context, the usage of digital technology in power distribution networks may provide significant pieces of information that can be helpful to reduce the complexity of this problem, with data gathered by PMUs communicating with the Distribution System Operator (DSO)[5] [6]. On the top of that, a methodology capable of detecting, identifying and isolating distinct events at distribution level such as power faults and voltage fluctuations may trigger automatic responses to provide self-healing or reconfiguration in order to reduce interruption times, improve quality of supply and optimize assets utilization[7] [8]. The main contribution of this paper fits into this context, as explained in the next sections.

PROPOSED EVENT DETECTION METHODOLOGY

The proposed methodology relies on a PCA algorithm to aggregate and evaluate statistically the PMU data recorded at the substation nodes[9] [10]. This method computes a statistical model that represents

1 M. Z. Jacobson, M. A. Delucchi, "Providing all global energy with wind, water, and solar power, Part I: Technologies, energy resources, quantities and areas of infrastructure, and materials," *Energy Policy*, vol. 39, no. 3, pp. 1154-1169, Mar. 2011.

2 M. Z. Jacobson, M. A. Delucchi, "Providing all global energy with wind, water, and solar power, Part II: Reliability, system and transmission costs, and policies," *Energy Policy*, vol. 39, no. 3, pp. 1170-1190, Mar. 2011.

3 R. F. Arritt and R. C. Dugan, "Review of the Impacts of Distributed Generation on Distribution Protection," in *2015 IEEE Rural Electric Power Conference*, Asheville, NC, 2015, pp. 69-74.

4 R. A. Walling, R. Saint, R. C. Dugan, J. Burke and L. A. Kojovic, "Summary of Distributed Resources Impact on Power Delivery Systems," in *IEEE Transactions on Power Delivery*, vol. 23, no. 3, pp. 1636-1644, July 2008.

5 V. C. Gungor *et al*., "Smart Grid Technologies: Communication Technologies and Standards," in *IEEE Transactions on Industrial Informatics*, vol. 7, no. 4, pp. 529-539, Nov. 2011.

6 R. E. Brown, "Impact of Smart Grid on distribution system design," 2008 IEEE Power and Energy Society General Meeting - Conversion and Delivery of Electrical Energy in the 21st Century, Pittsburgh, PA, 2008, pp. 1-4.

7 X. Fang, S. Misra, G. Xue and D. Yang, "Smart Grid — The New and Improved Power Grid: A Survey," in *IEEE Communications Surveys & Tutorials*, vol. 14, no. 4, pp. 944-980, Fourth Quarter 2012.

8 V. Telukunta, J. Pradhan, A. Agrawal, M. Singh and S. G. Srivani, "Protection challenges under bulk penetration of renewable energy resources in power systems: A review," in *CSEE Journal of Power and Energy Systems*, vol. 3, no. 4, pp. 365-379, Dec. 2017.

9 LL. Burgas, J. Melendez, J. Colomer, J. Massana, C. Pous, "Multivariate statistical monitoring of buildings. Case study: Energy monitoring of a social housing building." *Energy and Buildings* vol. 103, pp. 338-351, 2015.

the normal operating conditions (NOC) with a reduced number of variables (projection space) such that the correlation among variables is preserved[11] [12]. As a result, abnormal operating conditions (AOC) can be detected by projecting the subsequent observations onto the modeled space and analysing consistency of observations with respect to the NOC model.

Hence, the fault detection strategy is divided in two main steps described as follows:

1) Statistical model of normal operating conditions with dimensionality reduction

First, the statistical NOC model is built as an *n*-by-*m* matrix $\mathbf{X}_{\mathbf{NOC}}$ obtained from *n* samples collected over a finite time horizon of *m* distinct phasor quantities supposed to be centered (i.e. zero mean) and standardized (i.e. unit variance). Next, the eigenvalues and eigenvectors are calculated with eigendecomposition as the *m*-by-*m* matrices **Λ** and **V**, respectively, and dimensionality reduction is performed by retaining the eigenvectors associated with the *r* largest eigenvalues of **Λ**, which represents the major variability of the data, in an *m*-by-*r* projection matrix **P**. Then, the results of the projection are calculated as a score matrix **T** as follows in equation **(1)**

$$\boldsymbol{T} = \boldsymbol{X}_{NOC}\boldsymbol{P} \quad \textbf{(1)}$$

Additionally, the algorithm provides two statistical indexes that help to identify when an observation does not fit the model and consequently can be classified as an AOC: Hotelling's T^2 (T^2) and Square Prediction Error (SPE). The former computes the distance of an observation to the centre of the projection space using equation **(2)**, whereas the latter calculates the variation of an observation out of the projection space with equation **(3)**

$$T^2 = \boldsymbol{T}\Lambda^{-1}\boldsymbol{T}^T \quad \textbf{(2)}$$

$$\mathrm{SPE} = (\mathbf{X}_{\mathbf{NOC}} - \widehat{\mathbf{X}}_{\mathbf{NOC}})(\mathbf{X}_{\mathbf{NOC}} - \widehat{\mathbf{X}}_{\mathbf{NOC}})^{\mathrm{T}} \quad \textbf{(3)}$$

with the projected value of $\mathbf{X}_{\mathbf{NOC}}$ given by equation **(4)**

$$\widehat{\mathbf{X}}_{\mathrm{NOC}} = \mathbf{T}\mathbf{P}^{\mathbf{T}} \quad \textbf{(4)}$$

The statistical limits of **(2)** and **(3)** are given by equations **(5)** and **(6)**, respectively, according to the desired confidence level *α*.

$$\mathrm{T}^2_\alpha = \mathrm{F}_\alpha(\mathrm{r}, \mathrm{n}-\mathrm{r})\, {(\mathrm{n}^2-1)\mathrm{r}}\big/{\mathrm{n}(\mathrm{n}-\mathrm{r})} \quad \textbf{(5)}$$

$$\mathrm{SPE}_\alpha = \theta_1\left[{\mathrm{h}_0 \mathrm{c}_\alpha\sqrt{2\theta_2}}\big/{\theta_1} + 1 + {\theta_2 \mathrm{h}_0(\mathrm{h}_0-1)}\big/{\theta_1^2}\right]^{1/\mathrm{h}_0} \quad \textbf{(6)}$$

where $F_\alpha\,(r, n–r)$ is the critical point of the Fisher-Snedecor distribution function for *r* and *n-r* degrees of freedom and a significance level *α*, c_α is the value of the normal distribution function for the same significance level *α*, and the constants *θ* and h_0 are given by equations **(7)** and **(8)**

$$\theta_\mathrm{k} = \sum_{\mathrm{i}=\mathrm{r}+1}^{\mathrm{m}} \lambda_\mathrm{i}^\mathrm{k}, \mathrm{k} = \{1, 2, 3\} \quad \textbf{(7)}$$

$$\mathrm{h}_0 = 1 - {2\theta_1\theta_3}\big/{3\theta_2^2} \quad \textbf{(8)}$$

In this step, if the calculated values of **(2)** and/or **(3)** of any observation violate the statistical limits given by **(5)** and/or **(6)**, then it is tagged as an outlier, removed from $\mathbf{X}_{\mathbf{NOC}}$, and the statistical NOC model is re-built. It is supposed that $\mathbf{X}_{\mathbf{NOC}}$ does not contain a significant number of outliers, as a fault-free observation lies close to the centre of the projection space (i.e. $T^2 \approx 0$) and is negligible in the residual space (i.e. SPE ≈ 0).

2) Detection of abnormal operating conditions

10 M. Rafferty, X. Liu, D. M. Laverty and S. McLoone, "Real-Time Multiple Event Detection and Classification Using Moving Window PCA," in *IEEE Transactions on Smart Grid*, vol. 7, no. 5, pp. 2537-2548, Sept. 2016.

11 Y. Zhou, R. Arghandeh, I. Konstantakopoulos, S. Abdullah, A. von Meier and C. J. Spanos, "Abnormal event detection with high resolution micro-PMU data," *2016 Power Systems Computation Conference (PSCC)*, Genoa, 2016, pp. 1-7.

12 Y. Ge, A. J. Flueck, D. Kim, J. Ahn, J. Lee and D. Kwon, "Power System Real-Time Event Detection and Associated Data Archival Reduction Based on Synchrophasors," in *IEEE Transactions on Smart Grid*, vol. 6, no. 4, pp. 2088-2097, July 2015.

Once the statistical NOC model is defined, an AOC can be detected by projecting subsequent observations onto the modeled space and evaluating consistency of results with respect to the NOC model. This can be achieved by replacing $\mathbf{X}_{\mathbf{NOC}}$ with $\mathbf{X}_{\mathbf{AOC}}$ in equation **(1)**, using the result to calculate **(2)** and **(3)**, and finally, comparing the indexes with the values of **(5)** and **(6)**.

In this step, if the calculated values of **(2)** and/or **(3)** of any observation violate the statistical limits given by **(5)** and/or **(6)**, then it is tagged as a fault and the DSO is warned to perform further actions and clear it from the network.

CASE STUDY

The proposed methodology is tested in a real-based power distribution network simulated in Matrix Laboratory (MATLAB). It represents the substation Tallers Casadesus located in L'Esquirol, Catalunya, which consists of a primary distribution feeder with branches connecting the substation node to the customers (i.e. local energy producers and/or consumers). The distribution substation has 138,64 kW of contracted power from a 250-kVA transformer Yyn0 (400 V secondary), with industrial and residential energy consumption profiles, and distributed generation from solar photovoltaic panels.

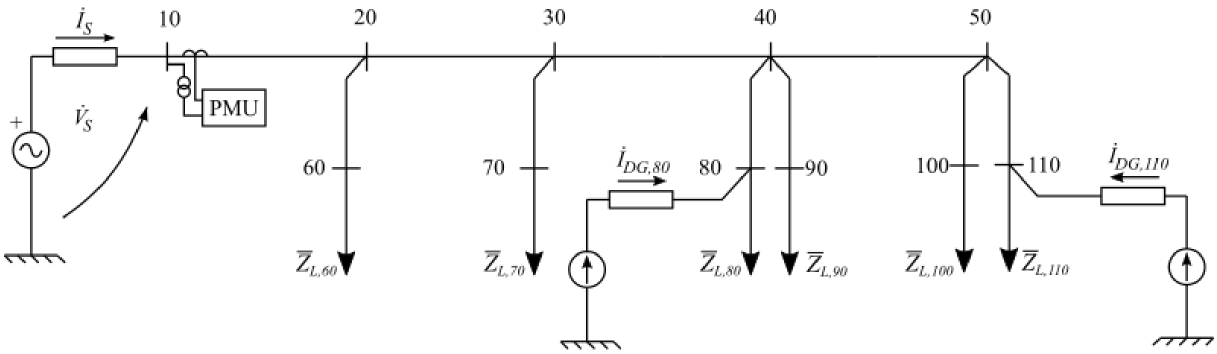

Fig. 1: Network topology with a single PMU installed at the substation node

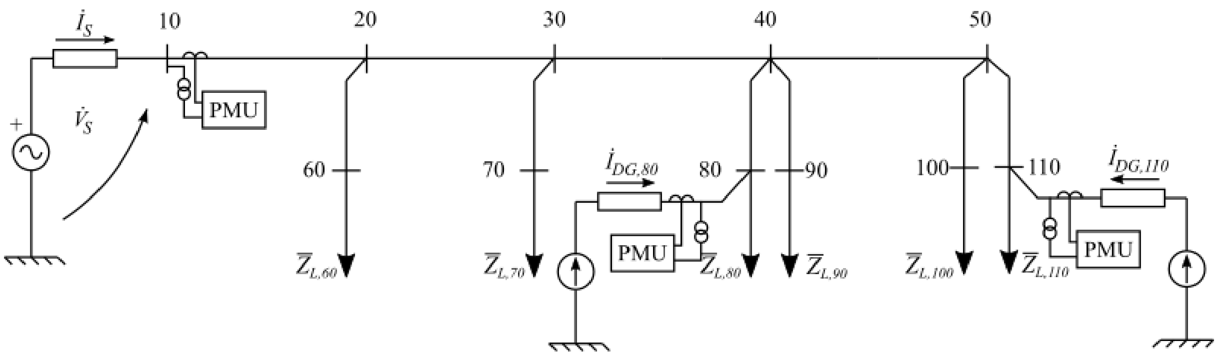

Fig. 2: Network topology with PMUs installed at the substation and distributed generation nodes

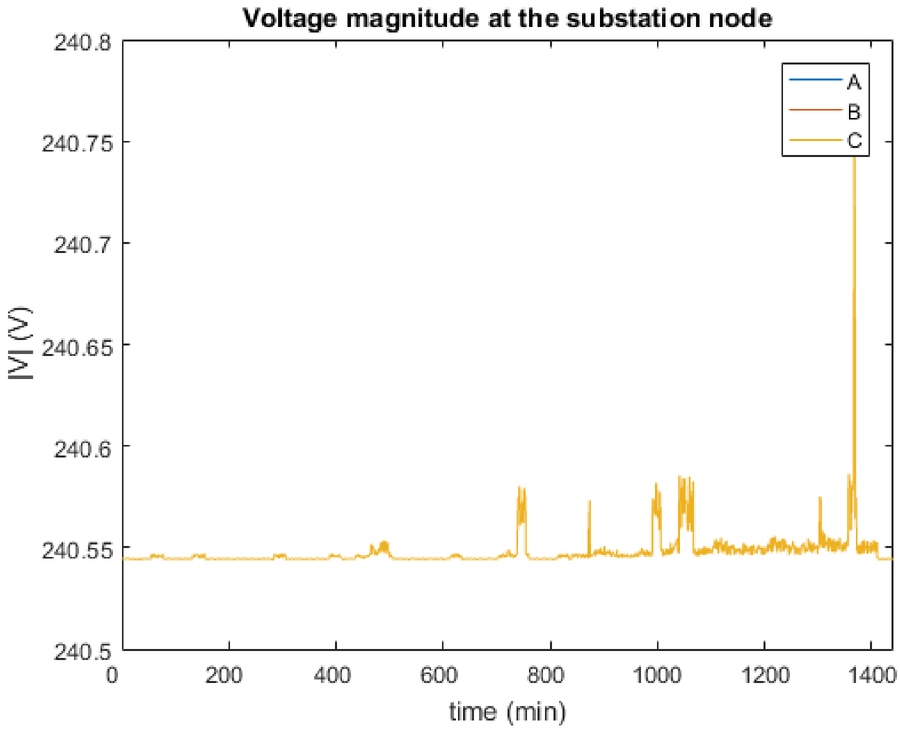

Fig. 3: Voltage magnitudes simulated at the substation node over a day

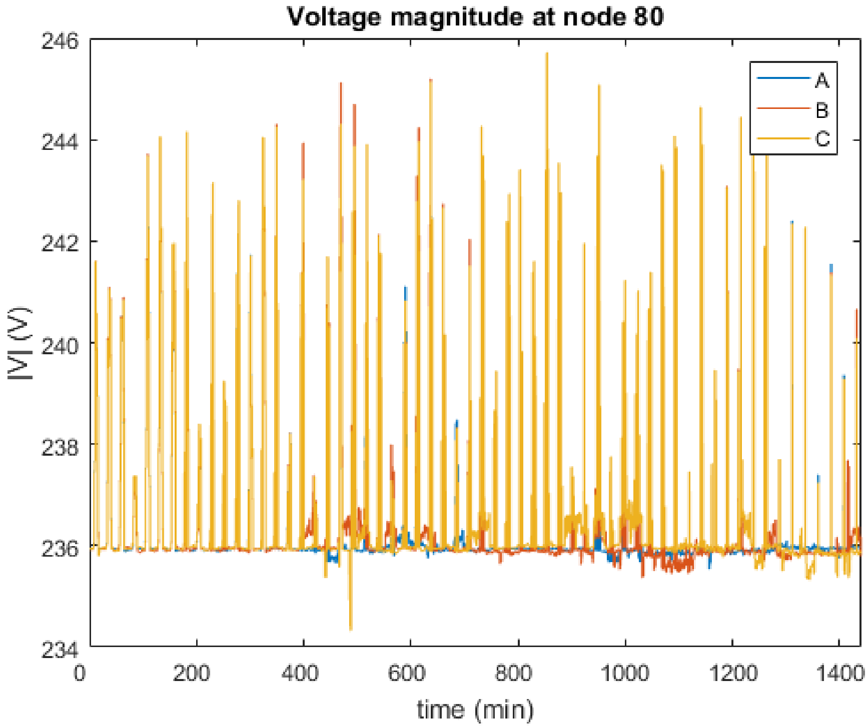

Fig. 4: Voltage magnitudes simulated at DG node 80 over a day

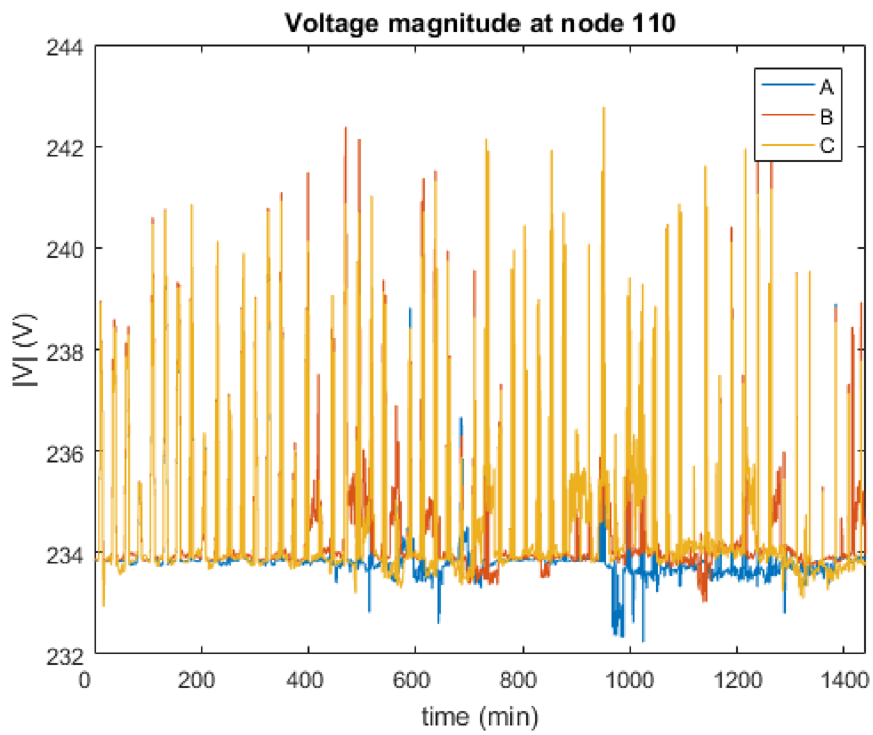

Fig. 5: Voltage magnitudes simulated at DG node 110 over a day

Two different PMU settings are evaluated: (1) a single PMU installed at the substation node (Fig.1); and (2) PMUs installed at the substation and DG nodes (Fig.2).

The statistical model is built with phase voltage magnitudes (in other words, m=3 in the 1st setting and m=9 in the 2nd setting) sampled every 100 milliseconds over a 1-day data frame window (with n=24x60x60x10=864000 samples per day), and tested under voltage sags and swells simulated sporadically. The voltage magnitudes recorded at the substation and DG nodes are illustrated in Fig.3, Fig.4, and Fig.5, respectively. The value of r is chosen r=1 with a single PMU installed and r=2 with multiple PMUs installed, as those principal component express over 99% of the total variability of faulty data in both PMU settings, whereas the values of $F_\alpha(r, n-r)$ and c_α are picked for α=0.95.

RESULTS

The calculated values of the T^2 and SPE indexes for phase voltage magnitudes when a single PMU is installed are illustrated in Fig.6 and Fig.7, respectively, together with their statistical limits, whereas the calculated values of the T^2 and SPE indexes for phase voltage magnitudes with PMUs installed at the substation and distributed generation buses are illustrated in Fig.8 and Fig.9, respectively, together with their statistical limits. It can be noticed that some values, associated with voltage sags and swells, present a different statistical pattern that surpasses the statistical limits and is clearly distinguishable from normal operation.

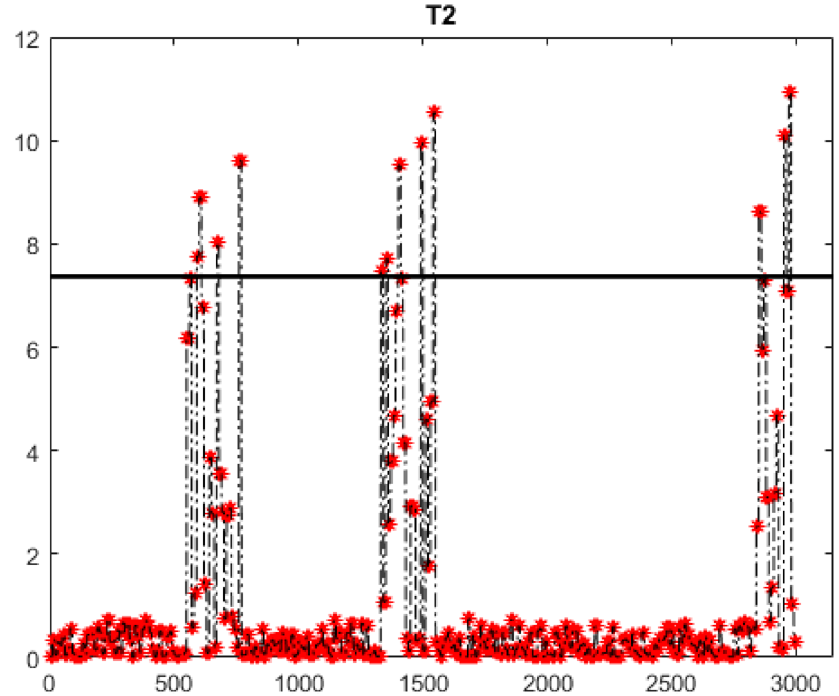

Fig. 6: T^2 index (red stars) and statistical limit (solid black line) with a single PMU installed

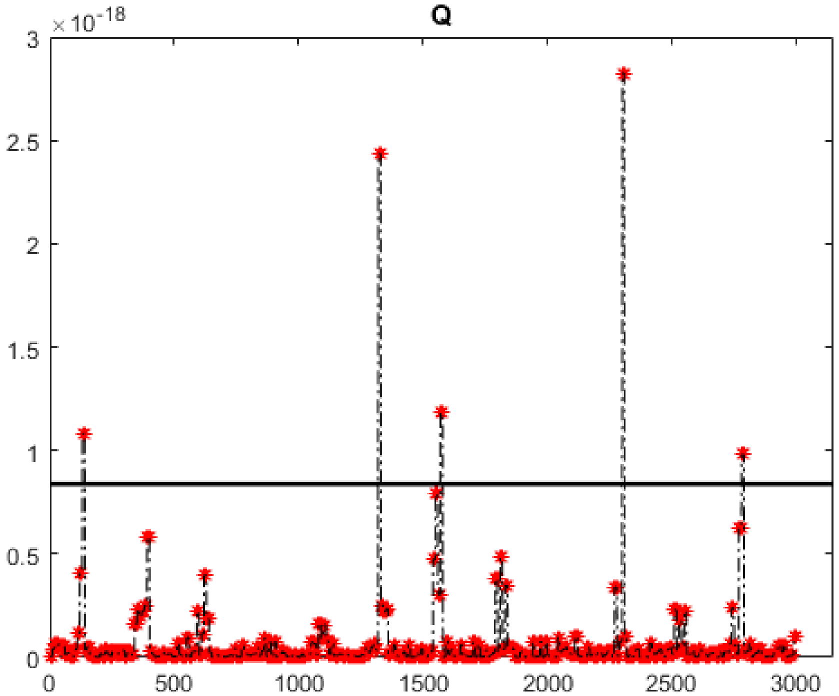

Fig. 7: SPE index (red stars) and statistical limit (solid black line) with a single PMU installed

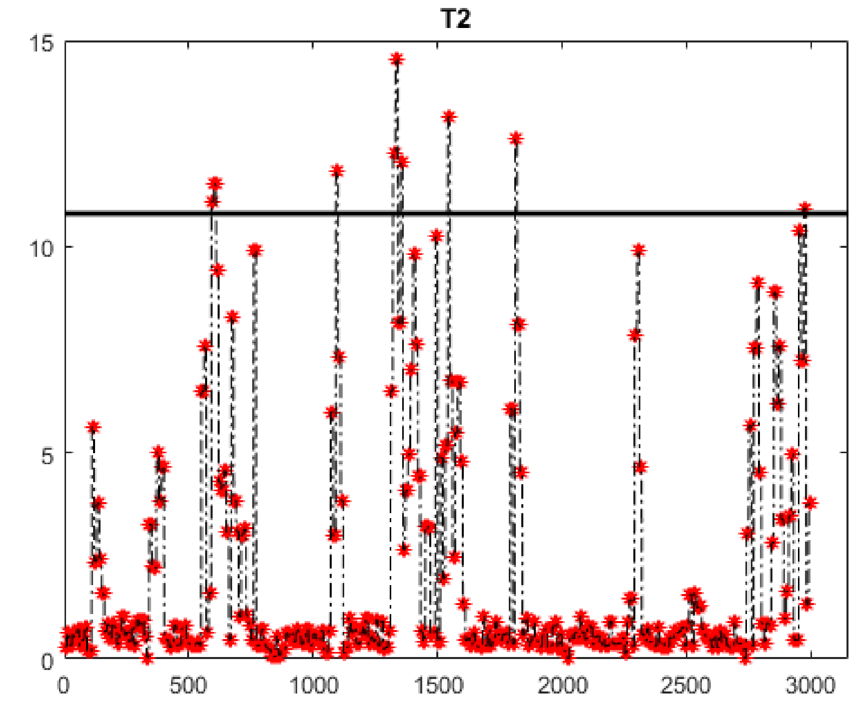

Fig. 8: T^2 index (red stars) and statistical limit (solid black line) with multiple PMUs installed

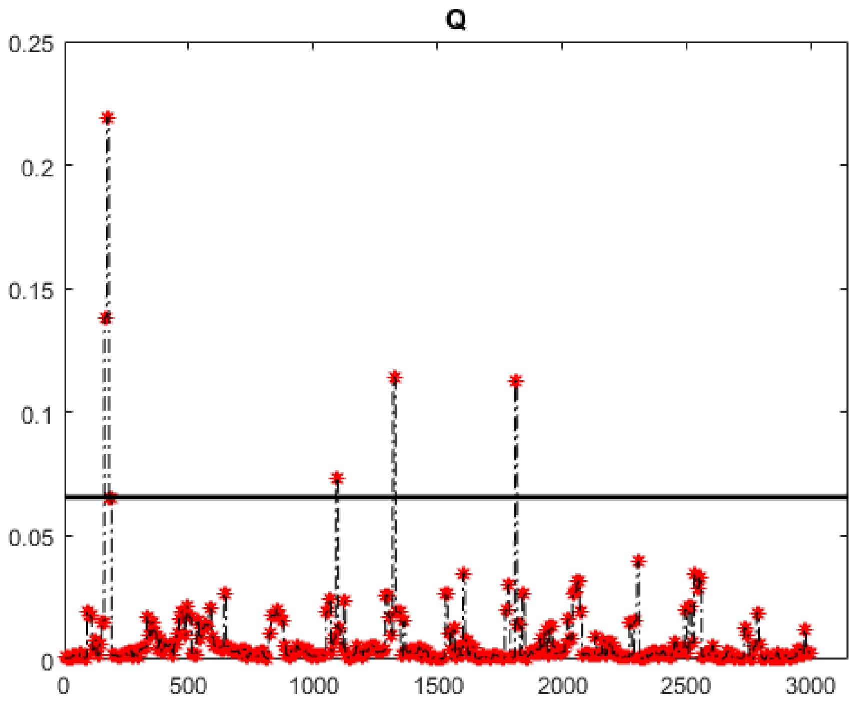

Fig. 9: SPE index (red stars) and statistical limit (solid black line) with multiple PMUs installed

DISCUSSION

The results show that the method is capable of detecting voltage sags and swells with both T^2 and SPE indexes with usage of distinct phasor quantities from NOC and AOC as input data. The combined usage of the T^2 and SPE indexes is thereby recommended to detect events in PMU data, as the results of individual event detections are not the same in all cases.

Although the SPE index is expected to perform better than the T^2 index due to the large variability of faulty data in the residual subspace, it only occurs in PMU setting (1) when it comes to the number of different event detections. The good performance of the T^2 index is due to the total variability of faulty data expressed in the projection space.

In addition, it can be noticed that the PCA model built with PMU setting (1) performs better than the PCA model built with PMU setting (2) with respect to the number of correct event detections with the SPE index and the time intervals of event detection with the T^2 index, but worse with respect to the number of correct event detections with the T^2 index. Also, it is noteworthy that the PCA model built with (1) is computationally more efficient than the PCA model built with (2), as it requires half the number of principal components to express the same variability of data, but provides a less accurate representation of the distribution network, as it does not include information about the DG nodes.

Moreover, it can be concluded from the choice of r that the model built with data collected by a single PMU is well represented by the eigenvector associated with the largest eigenvalue, as it represents a three-phase, symmetrical network. In turn, the model built with data collected by three PMUs is well represented by the eigenvectors associated with the two largest eigenvalues, as they represent a three-phase, symmetrical network with two different supply sources. As a result, faults can be easily detected with significant dimensionality reduction, as the number of variables is reduced from 3 to 1 with a single PMU installed and from 9 to 2 with three PMUs installed.

Furthermore, it is important to point out that the NOC model does not have to be adjusted to any changes in the energy production and consumption profiles, as the simulations are run in steady state. Consequently, the observation matrix does not have to be built or updated online to improve the situational awareness of the proposed methodology.

Further information about the network topology and electrical parameters of its components is not necessary to perform fault detection, albeit crucial to locate and diagnose faults.

CONCLUSIONS

The automated PCA-based event detection strategy is able to detect voltage sags and swells in low voltage distribution grids with DGs and PMUs with good accuracy. The results obtained with the T^2 and SPE statistical indexes allow for correct distinction between NOC and AOC in PMU data without requiring any information about the network topology or electrical parameters of its components. However, the PMU setting and the observation matrix may contribute to the task and shall be adjusted to different scenarios so that distinct faults can be detected.

ACKNOWLEDGEMENTS

This project has received funding from the European Union’s Horizon 2020 research and innovation framework under the auspices of the project “Renewable penetration levered by Efficient Low Voltage Distribution grids”, grant agreement number 773715.